Miniaturized Ozonolysis Flow Platform for Expeditious Sulfur Mustard Warfare Simulant Neutralization

Maxime Boddaert, Pauline Bianchi, Diana Silva-Brenes, Ancuta Musina, Marc Winter, Philippe Roth, Pierre-Yves Renard, Julien Legros, Jean-Christophe Monbaliu

Miniaturized Ozonolysis Flow Platform for Expeditious Sulfur Mustard Warfare Simulant Neutralization

Maxime Boddaert,[a,b,¶] Pauline Bianchi[a, ¶], Diana V. Silva-Brenes,[a,c] Daniel Courboin,[d] Marc Winter,[d] Philippe M. C. Roth,[d] Pierre-Yves Renard,[b] Julien Legros*[,b] and Jean-Christophe M. Monbaliu*[,a,c]

This communication introduces a highly efficient, safe and sustainable flow protocol for the oxidative neutralization of sulfur-based Chemical Warfare Agent simulants using ozone. The methodology employs preliminary *in silico* mechanistic studies and chemical analogy studies with DFT to scout reaction profiles and kinetics. It unveils crucial parameters that guide selectivity and prevent the formation of undesirable overoxidized by-products. This computational foundation is seamlessly translated into real-world neutralization experiments conducted under flow conditions, yielding remarkably swift neutralization rates under mild conditions. Full oxidative neutralization of CWA simulants with ozone is achieved within a second, without the need for additives or catalysts, in an EtOH/water mixture. This convergence of computational insights and experimental validation provides a promising avenue toward new neutralization protocols, foreseeing transformative possibilities with low waste generation and high safety.

Introduction

Bis(2-chloroethyl) sulfide (aka sulfur mustard, mustard gas, yperite, or **HD**; CAS 505-60-2) was originally prepared by Guthrie and Niemann in 1860.[1,2] It was first weaponized during World War I as a vesicant, inducing severe skin and mucous membrane blistering upon contact. Despite having already been prohibited from deployment on battlefields with Geneva Protocol (1925), the manufacture, accumulation, and utilization of **HD**, alongside other chemical warfare agents (CWAs), were subsequently proscribed by the Chemical Weapons Convention (CWC) in 1997. The Organization for the Prohibition of Chemical Weapons (OPCW) and the CWC-signatory countries have relentlessly worked on the destruction of existing stockpiles.[3,4] These endeavours reached their culmination with a recent declaration from the US Department of Defense, confirming the accomplished destruction of domestic CWA stockpiles.[5]

With these significant achievements in disarmament, the interest for developing new neutralization protocols specifically targeting **HD** can be legitimately questioned. There are, however, still other threatening scenarios involving **HD**. The few countries that have not ratified the CWC, on the one hand, and current geopolitical instabilities and terrorist threats on the other, are only visible part of the iceberg. A silent, background threat of unforeseeable ecological and societal magnitude lies in the many maritime dump sites of CWAs remnants from World Wars I & II.[6,7] All of the aforementioned points provide ample fuel for continued creative exploration aimed at enhancing the efficiency of neutralization, detection, and emergency protocols. Documentation of these research domains has been steadily growing.[8–13]

Neutralization and/or destruction protocols are designed to impede the formation of an electrophilic episulfonium species **epi-HD**, pertaining the acute toxicity of sulfur mustards (Figure 1a,b). The official method for destroying **HD** involves its direct incineration or the incineration of the corresponding hydrolysate after treatment under hot alkaline conditions.[14] Examples of solvolysis under hyperbaric conditions have also been reported,[15] as well as nucleophilic neutralization[16] and dehydrohalogenation

protocols.[17] Selective sulfoxidation is by far the most reported protocol in the primary literature. It has been described through a multitude of variants including either (photo)catalytic or stoichiometric conditions (Figure 1b).[10,11] Regardless of the conditions, the selectivity of the oxidation is the most critical parameter often at the expense of the atom economy, production costs, toxicity and practical considerations. Overoxidation to the corresponding toxic sulfone must be rigorously prevented (Figure 1b).

In a series of previous articles, we have documented our efforts to develop efficient oxidative neutralization flow processes specifically targeting **HD** simulants (e.g., **CEES** or **CEPS**).[18–21] We believe that such protocols are to rely on simple, widely available chemicals (Figure 1c) in order to facilitate their widespread adoption in emergency situations. Our efforts also aims low toxicity and safe process conditions. In addition, we have initiated innovation through the use of advanced computational methods, to both guide and further validate the neutralization processes on actual CWAs *in silico*.[18,21] Such a multidisciplinary approach offers safer and more sustainable options to address this challenging research area, with limited waste generation and chemical hazards for the operators.

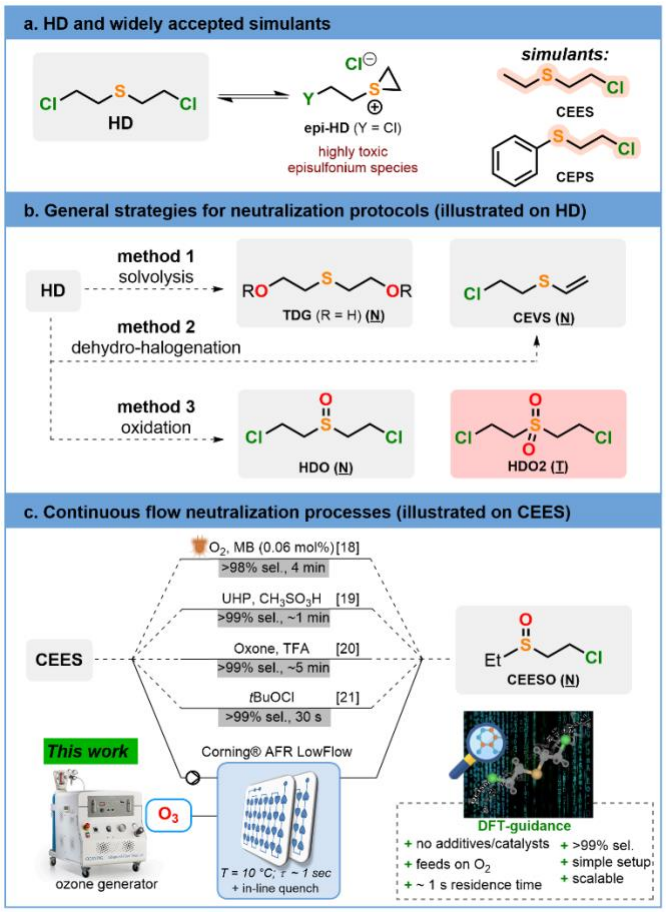

Fig. 1. Protocols for the chemical neutralization of **HD** and stimulants. (**N**) refers to neutralized, low toxicity species, while (**T**) refers to toxic byproducts. **(a)** Structure of **HD**, its toxic episulfonium derivative (**epi-HD**) and widely accepted lower toxicity simulants (**CEES** and **CEPS**). **(b)** General protocols for the neutralization of **HD** and simulants, including solvolysis, dehydrochlorination and oxidation. **(c)** Continuous flow oxidative neutralization processes using either (photo)catalytic or stoichiometric conditions. The main strategy presented in this communication is illustrated.

In this communication, we present a highly effective and sustainable protocol for the oxidative neutralization of **HD** simulants utilizing ozone under continuous flow conditions. The generation of ozone directly from compressed air/oxygen obviates the need for supplementary additives or catalysts, thereby harnessing its inherent oxidative potential to the fullest extent. Our initial exploration encompassed *in silico* analyses using a DFT protocol, elucidating the mechanism,

selectivity, and intrinsic features. Additionally, we illustrate a rational selection process for low toxicity simulants of **HD**, employing conceptual DFT to identify thioethers with analogous chemical behavior while mitigating the proscribed nature and toxicity associated with **HD**. Computational profiles and kinetics of reactions *in silico* were computed to emphasize the most influential parameters driving selectivity and preventing the formation of toxic overoxidized by-products (sulfone derivatives). The computational work is next translated to actual neutralization experiments conducted under flow conditions, yielding unprecedently fast neutralization rates (full neutralization within a mere second).

Experimental Section

General information

Conversion, selectivity, and yield were determined by Gas Chromatography coupled to Flame Ionization Detection (GC-FID) or Mass Spectrometry (GC-MS) or by High Performance Liquid Chromatography coupled to Diode-Array Detection (HPLC-DAD) or coupled with Mass Spectrometry (LC-MS). Conversion stands for the amount of sulfide consumed while yield is defined as the amount of sulfoxide produced. Structural identity was confirmed by ^{1}H and ^{13}C NMR spectroscopy (400 MHz Bruker Avance spectrometer), by LC-MS or GC-MS (Supporting Information, Section 6). Methyl phenyl sulfide (**1a**), methyl phenyl sulfoxide (**2a**), methyl phenyl sulfone (**3a**), dipropyl sulfide (**1b**), dipropyl sulfoxide (**2b**), dipropyl sulfone (**3b**), 2-chloroethyl phenyl sulfide (**CEPS**), 2-chloroethyl ethyl sulfide (**CEES**), ethanol, water, sodium thiosulfate were purchased from commercial sources and used without additional purification (Supporting Information, Section 3.1.). **CEPSO, CEPSO$_2$, CEESO and CEESO$_2$** and were prepared according by adapting protocols from the literature.[22,23]

Computational study

Calculations were performed using the Gaussian 16[24] package and implicit solvation (SMD, solvent = ethanol). Optimization and characterization with vibrational analysis of the stationary points were carried out at the B3LYP-D3BJ/6- 31+G* level of theory. Electronic energies were computed at the M08HX/6-311+G** level whereas solvation energies and Gibbs free energy corrections were obtained at the B3LYP-D3BJ/6-31+G* level. Computations of the activation barriers corrected by concentration and quasi-harmonic factors (Grimme method for entropy and Head-Gordon method for enthalpy correction),[25] as well as reaction times, were performed using our open-access SnapPy toolkit (v1.0.0.).[26] Transition states (TSs) were determined with the Newton−Raphson technique, then checked with the Hessian matrix and intrinsic reaction coordinates (IRC). The lowest energy conformation for each transition state was kept for determining activation barriers. NBO charges were calculated using the NBO 3.1 extension from Gaussian. Local nucleophilicity on the sulfur atom was calculated using equations from conceptual Density Functional Theory.[27,28] All equations and the protocols followed are available in the Supporting Information (Section 1.1).

Safety statement

CAUTION: 2-chloroethyl phenyl sulfide (**CEPS**) and 1-chloro-2-(ethylsulfinyl)ethane (**CEES**) are highly toxic and severe vesicants and must be handled under a fume hood. All contaminated glassware should be neutralized with bleach prior to disposal. Ozone is a toxic and strong oxidizer. All experiments should be carried out under a fume hood in the presence of a fully qualified ozone detector. For additional safety, it is recommended that the operator possesses a portable personal ozone detector at all times during operations. Ozone can also form peroxides with various organic compounds; it is recommended to regularly use peroxide test strips on reactor effluents before disposal. Ozone decomposes with the formation of oxygen, therefore potentially forming a flammable oxygen/solvent mixture. To mitigate this risk, it is strongly recommended to degas and dilute the reactor effluent with a continuous stream of nitrogen. Additional details on the safety measures are detailed in the Supporting Information (Section 4). The readers should become aware of legal restrictions in their country on the permittance to study **HD** or any

related analogs of chemical warfare agents before possessing them in the lab.

Optimized conditions for the oxidative neutralization of CEES

Lab scale mesofluidic experiments were carried out in a Corning® Advanced-Flow™ LowFlow Reactor (0.5 mL internal volume glass fluidic modules; 2 fluidic modules connected in series) connected to a Corning Ozone generator. Liquid feeds were handled with syringe or piston pumps (Knauer – Azura P4.1S for the feed solution A; HiTec Zang SyrDos™ 2 XLP for feed solution B). Feed and collection lines consisted of PFA tubing (1/8" o.d.) with PFA or SS Swagelok connectors and ferrules. The process temperature was regulated with a LAUDA PROLINE RP 845 thermostat. The downstream pressure was set at 7 bar (Zaiput BPR-10). The reactor setup was thoroughly flushed with nitrogen, and then with 1:1 EtOH/H_2O mixture for 5 min. The pump handling feed solution B (0.2 M sodium thiosulfate quench solution in 9:1 (*v:v*) water/ethanol mixture) was set to XX mL min^{-1} prior to feeding upstream the reactor with ozone (800 mL_N min^{-1}). Lastly, the pump handling feed solution A (0.5 M **CEES** in EtOH) was set to XX mL min^{-1}. **CEES** was reacted with ozone at 0 °C for a residence time of 1 s. Samples were collected at steady state.

Results and Discussion

Computational design

The access to **HD** is restricted to very few labs worldwide with military clearance. While such restriction is perfectly understandable given all the above, it is clearly a main limitation when it comes to the development of actual **HD** neutralization protocols. Surely, just safety reasons are enough to trigger the search for alternative, low-toxicity structures, yet able to provide relevant chemical information. There is a wide range of thioethers commercially available, and among them, both **CEPS** and **CEES** are commonly used **HD** simulants for obvious structural resemblance**.** However, both compounds are toxic and severe vesicants, the use of which should not be taken lightly for the development of neutralization processes. Other suitable thioethers may be commercially available, pending that sufficient and quantitative information is available to make them eligible as potential simulants. In an ideal scenario, a low toxicity, widely available thioether would be used to develop new process conditions, prior to transposition to a closer **HD** simulant. The access of such a quantitative metric to claim chemical analogy with **HD** can be accessed *in silico*. The availability of the non-bonding n_S orbitals through stereoelectronic interactions has been already proposed by our lab as a first metric to rank the potential candidates,[18] though it provided only a guesstimate approach. Meanwhile, we have developed the necessary tools and know-how for accessing a more refined selection protocol. The latter relies both on Conceptual Density Functional Theory (CDFT)[27,28] and on the accurate calculation of activation barriers through our open-source software.[26] The combination of both provided a powerful tool for extracting relevant chemical information towards chemical analogy. We believe that the increasing reliance on *in silico* methods to predict chemical behavior can also contribute in reducing the amount of waste generated upon experimental trial-and-error and optimization phases, specifically when toxic compounds are involved.[29]

In the presence of ozone, the sulfur atom of **HD** is expected to behave as a nucleophile,[30] which is confirmed with the computations of the reaction mechanism (see below). Therefore, the local nucleophilicity (N_S)[27] on the sulfur atom of **HD** and six potential simulants was computed at the B3LYP-D3BJ/6-31+G* level in ethanol (Figure 2a) using a classical approach in CDFT. The six potential thioether simulant candidates included methyl phenyl sulfide (**1a**), dipropyl sulfide (**1b**), diphenyl sulfide (**1c**), dibenzo[b,d]thiophene (**1d**), 2-chloroethyl phenyl sulfide (**CEPS**) and 2-chloroethyl ethyl sulfide (**CEES**).

The local nucleophilicity on **1b** (N_S = 2.1) emphasizes a stronger nucleophilic behavior than the other computed thioethers. Conversely, **1c** (N_S = 1.0) and **1d** (N_S = 0.8) appeared at the antipode, their nucleophilicity being reduced through delocalization. **CEES** (N_S = 1.9), **1a** (N_S = 1.8) and

CEPS (N_S = 1.6) demonstrated local nucleophilicities akin to **HD** (N_S = 1.8). This initial analysis underscores **1a** and **CEES** as the closest **HD** simulants in terms of local nucleophilicity. Refining the analysis through the computation of Molecular Electrostatic Potential (MEP) surfaces corroborated the CDFT trends. MEP surfaces also reveal the intense electron-withdrawing effect of chlorinated substituents (Figure 2a), thus providing more insight into the necessary requirements to mimic the reactivity of **HD**. From there, it became apparent that **1a** is a promising simulant for **HD**, given its low toxicity compared to **CEES**. While being structurally different, it mimics the nucleophilicity of the sulfur atom on **HD** yet it lacks its activated C-Cl bond. **CEES** is therefore the most trustworthy simulant, combining both similar sulfur local nucleophilicity and at least the influence of one activated C-Cl bond. On the other hand, despite structural proximity to **CEES**, **CEPS** does not emerge as an optimal simulant, with a decreased N_S, and likely entails distinct chemical behavior.

The relevance of the sulfur local nucleophilicity as a suitable metric for the selection of **HD** simulants was further validated *in silico*. Transition states associated with the oxidation of thioethers **1a-d**, **CEPS, CEES** and **HD** were computed in EtOH toward the corresponding sulfoxides **2a-d**, **CEPSO, CEESO** and **HDO**, as well as for the undesired overoxidation to sulfones **3a-d**, **$CEPSO_2$, $CEESO_2$** and **HDO_2** (Figures 2a,b and Supporting Information, Sections 1.3 and 1.4). The corresponding activation barriers ($\Delta G^{\neq}$) follow a similar trend to the local nucleophilicity index, as illustrated in Figure 2a. As a general trend, the higher the sulfur local nucleophilicity, the lower the activation barrier, at least for the critical sulfoxidation. These activation barriers can be connected to inherent kinetics through Eyring's equation (Supporting Information, Section 1.1). For the sulfoxidation, the oxidations of all thioether substrates are characterized by low activation barriers ($\Delta G^{\neq}$ <8 kcal mol^{-1}), which translates to reaction completion below 1 s (at 10 °C and 0.2 M). The overoxidation to the undesired sulfones comes with a higher activation barrier, at least for substrates **1a,b**, **CEPS**, **CEES** and **HD** (3.1 < $\Delta\Delta G^{\neq}$ < 6 kcal mol^{-1}). For compounds **1c,d**, the overoxidation appears to be more favorable than the sulfoxidation by 0.5-0.8 kcal mol^{-1}. Nevertheless, computational results confirm, in all instances, the selectivity issues : activation barriers for overoxidation also translate into extremely fast kinetics, with 99% conversion expected below 1 s under the same conditions. It can therefore be concluded that these reactions are clearly limited by diffusion ($Da > 1$)[31] and require high mixing efficiency to avoid concentration gradients. Selectivity towards the sulfoxide will therefore critically depend on both the selection of an appropriate setup allowing for short reaction times and high mixing efficiency, as well as an appropriate quenching of any remaining ozone. This scenario emphasizes a case where conventional batch protocols encounter challenges in fulfilling these criteria. Furthermore, batch ozonolysis typically demands sub-zero temperatures to mitigate the potential for explosive reactions. This sustained our endeavor toward a development under flow conditions, where dedicated flow reactors are meticulously engineered to sustain optimal mixing efficiency. Both the ability to integrate *in situ* quenching capabilities and the absence of headspace are also foreseen as important safety features for potentially flammable and/or explosive mixtures.[32]

Experimental validation

There is precedent for the ozonolysis under continuous flow (micro and mesofluidic setups) on various substrates.[33–39] Here, experiments were performed using a commercial Corning® Advanced-Flow™ Reactor (AFR) specifically designed for a minimal footprint (AFR™ LowFlow). The reactor configuration featured 2 LowFlow glass fluidic modules (FM, 0.5 mL internal volume each) specifically designed for high mass transfer in liquid-gas biphasic systems. Both FMs were fluidically connected in series and featured an embedded high-performance heat exchanger. The reactor setup was fed upstream with compressed ozone (10 bar) and with a liquid feed of thioether

in ethanol. FM1 was used for the oxidation of various **HD** thioether simulants with ozone, while FM2 was used to quench the reaction mixture (aqueous sodium thiosulfate, 0.2 M). The pressurized ozone generator has been reported elsewhere.[33] Note here that the in-line quench is an additional safety feature to neutralize any unreacted ozone prior to the collection of reaction effluents. The reactor effluents were analyzed either by HPLC or GC-FID (ESI, see Section 3.2). Optionally, an in-line benchtop NMR (benchtop Spinsolve 43 Carbon Ultra) can be used for qualitative reaction monitoring. A simplified flow chart for the ozone neutralization platform is depicted in Figure 3 (refer to the ESI, section 4 for a detailed setup and experimental protocols, pictures and risk analysis).

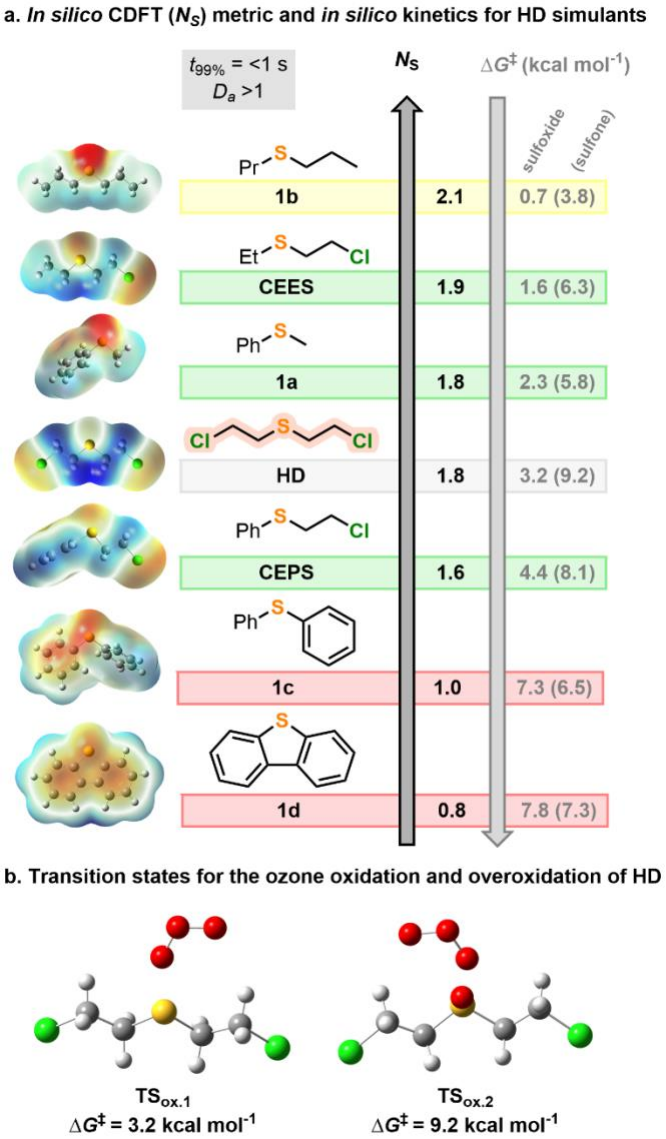

Fig. 2. (a) *In silico* **HD** simulant selection at the B3LYP/6-31+G*//M08HX-6-311+G** level (SMD = EtOH) (Supporting Information, section 1.2). *N*s refers to the local nucleophilicity at the sulfur atom; $\Delta G^{\ddagger}$ to the activation barrier for the sulfoxidation and the overoxidation to sulfone (in brackets); $t_{99\%}$ to the time to reach 99% conv. of the substrate at 0.2 M and 10 °C; *Da* to the Damköhler number. Inserts on the left handside depict the Molecular Electrostatic Potential (MEP) surfaces (in red: negative potential up to -0.03 au, in blue: positive potential up to 0.03 au). Colour code: green, good simulants for **HD**; yellow, average simulant for **HD**; red, poor simulants. **(b)** Transition state structures (B3LYP/6-31+G*) and activation energies for the oxidation of **HD** toward

HDO and **HDO₂** (Supporting Information, section 1.3 and 1.4).

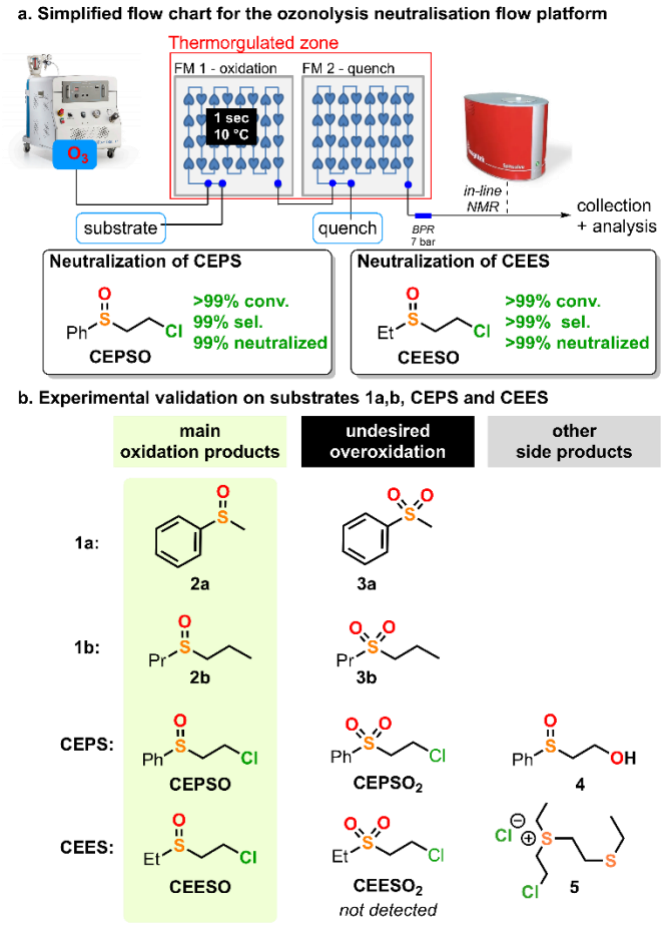

Fig. 3. (a) Simplified flow chart. **(b)** Structure from the different products formed upon ozone oxidation on compounds **1a,b, CEPS** and **CEES** on the crude reactor effluents (see Table 1). Feed solutions for compounds **1a,b, CEPS** and **CEES** were prepared in EtOH (0.2 or 0.5 M, see Table 1). The reactor effluent was quenched with 0.2 M aqueous sodium thiosulfate. All experiments were monitored with an ozone detector at the outlet of the reactor.

Preliminary experiments started with **1a** to calibrate our system with the computational study (0.2 M in EtOH). A controlled experiment where the feed of ozone was replaced with pure oxygen led to no conversion. With 1.5 equiv. of ozone, full conversion of **1a** into its corresponding sulfoxide **2a** was achieved within 1 s of residence time at 10 °C (Figure 3, Table 1, Entry 1). The selectivity of the oxidation was total, with no detectable traces of the corresponding sulfone **3a**. With these promising results in hand, we transitioned to the oxidation of **1b** (Figure 3, Table 1, Entry 2). Under the same conditions, full conversion was obtained. The selectivity, however, was lower with the formation of about 4% of the overoxidized sulfone **3b** along with the desired sulfoxide **2b** (96%). The overoxidation is not surprising in light of the preliminary computational study, which emphasized the higher nucleophilicity of **1b**.

Next, our focus shifted towards the oxidation of **CEPS** and **CEES**, both being commonly reported as simulants of **HD**. As outlined in the initial computational exploration, the experimental observations further reflected that **CEPS** has a different behavior than **CEES.** Altogether, it emphasizes **CEES** as a much better simulant of **HD**. When the oxidation was carried out on **CEPS** with a substoichiometric amount of ozone (0.8 equiv), conversion barely reached 80% (35% yield towards sulfoxide **CEPSO**)(Entry 3). Under these conditions, the major product became hydrolysate **4** (41 %). The hydrolysis occurred in the quench FM and consumed all unreacted **CEPS**. Increasing the excess of ozone to 1.4 equiv. led to a 91% conversion (Entry 4) and a 88% yield towards **CEPSO** (2% **CEPSO₂** detected in the crude). When the concentration of the feed solution of **CEPS** was increased up to 0.5 M, total conversion and a selectivity of 99% toward **CEPSO** was achieved with 1.5 equiv. of ozone (Entry 5).

Table 1. Oxidative neutralization with ozone under flow conditions (see Figure 3).

Entry	***Substrate*** [a] ***(M)***	***Ozone (equiv.)***	***Conv.*** [b] ***(%)***	***Yield*** [c] ***(%)***	***Other Products (%)***
1	**1a** (0.2)	1.5	>99	>99	/
2	**1b** (0.2)	1.5	>99	96	**3b** (4)
3	**CEPS** (0.2)	0.8	80	35	**CEPSO₂** (4) **4** (41)
4	**CEPS** (0.2)	1.4	91	88	**CEPSO₂** (2) **4** (1)
5	**CEPS** (0.5)	1.5	>99	99	**CEPSO₂** (1)
6	**CEES** (0.2)	0.8	>99	84	**5** (16)

7	**CEES** (0.2)	1	>99	>99	/
8	**CEES** (0.2)	1.5	>99	>99	/
9	**CEES** (0.5)	1	>99	>99	/

[a] All experiments were carried out at 10 °C with a backpressure of 7 bar. All samples were quenched with aqueous sodium thiosulfate (0.2M). Data from LC (**1a**, **CEPS**) or GC-FID (**1b**, **CEES**) analysis. [b] Amount of sulfide **1a**, **2a**, **CEPS** or **CEES** consumed. [c] Amount of the corresponding sulfoxide **2a**, **2b**, **CEPSO** and **CEESO** produced.

As a final demonstrator, the oxidation process was attempted on **CEES** (0.2 M in EtOH). With a substoichiometric amount of ozone (0.8 equiv.), full conversion of **CEES** was already achieved, with a very high selectivity toward **CEESO** (84%). The undesired sulfone **$CEESO_2$** was barely detected (<1%), while the main side-product (16%) was the dimeric salt **5**. This result clearly contrasts with **CEPS** under similar experimental conditions, where the amount of sulfone is higher (4%), and the main by-product is hydrolysate **4**. In the case of **CEES**, the corresponding hydrolysate is not observed under our conditions. With a stoichiometric amount of ozone, full conversion was attained. Most importantly, total selectivity (>99%) was obtained for the desired sulfoxide **CEESO**. Interestingly, a slight excess of ozone did not degrade the selectivity (up to 1.5 equiv.). Finally, the concentration of the feed solution of **CEES** could be increased (0.5 M in EtOH) while maintaining full conversion and selectivity within 1 s.

In a controlled experiment where the residence time was increased to 10 s (achieved through adjustments in the configuration of the flow setup with several additional FMs), the results indicate overoxidation (68% of **$CEESO_2$** and 39% for **$CEPSO_2$**) at 10 °C. These results not only highlight the potent oxidizing power of ozone but also align closely with the calculated selectivity, underscoring the critical need of minimizing residence times to uphold desired selectivity levels.

Conclusion

We have developed an innovative protocol for the oxidative neutralization of **HD** simulants with unprecedented efficiency (0.5 M and 1 s residence time). This procedure harnesses the benefits of continuous flow to maximize the potent oxidizing nature of ozone. The methodology incorporates an initial DFT study to rationally guide the selection of appropriate simulants for HD oxidative neutralization processes and collect critical information on kinetics and selectivity, while preventing the generation of unnecessary waste compounds. We demonstrate the relevance of the local nucleophilicity on sulfur as a metric for ranking simulants. As far as oxidative pathways are concerned, methyl phenyl sulfide (**1a**) appears as a good simulant with low toxicity for preliminary scouting of reaction conditions. Among two of the most widely used simulants, namely, 2-chloroethyl phenyl sulfide (**CEPS**) and 2-chloroethyl ethyl sulfide (**CEES**), CFDT descriptors clearly emphasize **CEES** as the best pick. We have also demonstrated how *in silico* kinetics can be generated to frame experimental conditions and to highlight the critical parameters to be taken into consideration for efficient and selective processes. The sulfoxidation of selected thioethers proceed with extremely fast kinetics primarily driven by diffusion. Subsequently, we successfully transitioned to a compact and efficient setup that guarantees optimal mixing, short residence times, and superior selectivity. This integrated configuration incorporates an in-line quench, enabling the selective oxidation of the designated simulants (>99% conversion to non-toxic sulfoxide species). Under these conditions, overoxidation toward the toxic sulfone only occurred significantly for diisopropyl sulfide (**1b**), which exhibits a much higher sulfur local nucleophilicity. This protocol herein described appears as one of the safest, most sustainable and compact oxidative neutralization processes: it uses mild conditions (10 °C, 7 bar of counterpressure), relies on EtOH/water as a solvent, and requires neither an additive nor a catalyst. This approach can be seamlessly integrated with widely accessible industrial ozone generators. The convergence

between computations and experiments is a promising tool for accessing meticulously designed protocols, substantially reducing contact with highly toxic compounds. These findings hold substantial promise for their extension to the neutralization of sulfur mustard.

Author Contributions

MB performed the experiments. PB designed and performed the computational study, analyzed the results and prepared the corresponding section in the manuscript and Supporting Information. DVSB supervised the experiments, wrote the experimental sections of the Supporting Information and proofread the manuscript. DC, MW and PMCR commissioned the mesofluidic reactor setup and the ozone generator, technically assisted for the experimental optimization and proofread the manuscript. JL and PYR designed the experiments and corrected the manuscript. JCMM designed the experiments, supervised the research and wrote the manuscript.

Conflicts of interest

There are no conflicts to declare.

Acknowledgements

Computational resources were provided by the "Consortium des Équipements de Calcul Intensif" (CÉCI), funded by the "Fonds de la Recherche Scientifique de Belgique" (F.R.S.-FNRS) under Grant No. 2.5020.11a and by the Walloon Region. PB is a F.R.S.-FNRS PhD fellow (ASP PhD fellowship 1.A.054.21F). This work was supported by the University of Liège, the F.R.S.-FNRS (Incentive grant for scientific research MIS F453020F, JCMM)., and Corning SAS. The authors also thank Labex SynOrg (ANR-11-LABX-0029), Carnot Institute I2C, the graduate school for research XL-Chem (ANR-18-EURE-0020 XL CHEM) and the Région Normandie.

Notes and references

1 F. Guthrie, *Q. J. Chem. Soc. London*, 1860, **12**, 109–126.

2 A. Niemann, *Justus Liebigs Ann. Chem.*, 1860, **113**, 288–292.

3 UNODA, Chemical Weapons, https://disarmament.unoda.org/wmd/chemical/, (accessed 20 August 2023).

4 OPCW, What is a Chemical Weapon?, https://www.opcw.org/our-work/what-chemical-weapon, (accessed 20 August 2023).

5 United States Government, US Completes Chemical Weapons Stockpile Destruction Operations, https://www.defense.gov/News/Releases/Release/Article/3451920/us-completes-chemical-weapons-stockpile-destruction-operations/, (accessed 20 August 2023).

6 I. Wilkinson, Chemical Weapon Munitions Dumped at Sea: An Interactive Map | James Martin Center for Nonproliferation Studies, https://nonproliferation.org/chemical-weapon-munitions-dumped-at-sea/, (accessed 20 August 2023).

7 H. Sanderson, P. Fauser, M. Thomsen, P. Vanninen, M. Soderstrom, Y. Savin, I. Khalikov, A. Hirvonen, S. Niiranen, T. Missiaen, A. Gress, P. Borodin, N. Medvedeva, Y. Polyak, V. Paka, V. Zhurbas and P. Feller, *Environ. Sci. Technol.*, 2010, **44**, 4389–4394.

8 P. Kalita, R. Paul, A. Boruah, D. Q. Dao, A. Bhaumik and J. Mondal, *Green Chem.*, 2023, **25**, 5789–5812.

9 C. R. Jabbour, L. A. Parker, E. M. Hutter and B. M. Weckhuysen, *Nat. Rev. Chem.*, 2021, **5**, 370–387.

10 E. Oheix, E. Gravel and E. Doris, *Chem. - A Eur. J.*, 2021, **27**, 54–68.

11 B. Picard, I. Chataigner, J. Maddaluno and J. Legros, *Org. Biomol. Chem.*, 2019, **17**, 6528–6537.

12 P. Kalita, R. Paul, C. W. Pao, R. Chatterjee, A. Bhaumik and J. Mondal, *Chem. Commun.*, 2023, **59**, 5067–5070.

13 M. Yu, J. Liu, F. Liu, F. Zou, L. Zhang and Q. Gao, 2023, **4**, 1–7.

14 A. C. W. Alternatives, Program Executive Office, https://www.peoacwa.army.mil/, (accessed 20 August 2023).

15 S. Mansour, V. B. Silva, E. S. Orth and J. Legros, *Org. Biomol. Chem.*, 2022, **20**, 7604–7608.

16 V. B. Silva, S. Mansour, A. Delaune, F.-X. Felpin and J. Legros, *React. Chem. Eng.*, 2023, Advance Article, DOI:10.1039/d3re00264k.

17 G. W. Wagner, P. W. Bartram, O. Koper and K. J. Klabunde, *J. Phys. Chem. B*, 1999, **103**, 3225–3228.
18 N. Emmanuel, P. Bianchi, J. Legros and J.-C. M. Monbaliu, *Green Chem.*, 2020, **22**, 4105–4115.
19 B. Picard, B. Gouilleux, T. Lebleu, J. Maddaluno, I. Chataigner, M. Penhoat, F. X. Felpin, P. Giraudeau and J. Legros, *Angew. Chemie - Int. Ed.*, 2017, **56**, 7568–7572.
20 A. Delaune, S. Mansour, B. Picard, P. Carrasqueira, I. Chataigner, L. Jean, P. Y. Renard, J. C. M. Monbaliu and J. Legros, *Green Chem.*, 2021, **23**, 2925–2930.
21 V. E. H. Kassin, D. V. Silva-Brenes, T. Bernard, J. Legros and J. C. M. Monbaliu, *Green Chem.*, 2022, **24**, 3167–3179.
22 J. Singh, T. P. Kissick and R. H. Mueller, *Org. Prep. Proced. Inc*, 1989, **21**, 501–504.
23 Y. Yuan, X. Shi and W. Liu, *Synlett*, 2011, **4**, 559–564.
24 Gaussian 16, Revision C.01, M. J. Frisch, G. W. Trucks, H. B. Schlegel, G. E. Scuseria, M. A. Robb, J. R. Cheeseman, G. Scalmani, V. Barone, G. A. Petersson, H. Nakatsuji, X. Li, M. Caricato, A. V. Marenich, J. Bloino, B. G. Janesko, R. Gomperts, B. Mennucci, H. P. Hratchian, J. V. Ortiz, A. F. Izmaylov, J. L. Sonnenberg, D. Williams-Young, F. Ding, F. Lipparini, F. Egidi, J. Goings, B. Peng, A. Petrone, T. Henderson, D. Ranasinghe, V. G. Zakrzewski, J. Gao, N. Rega, G. Zheng, W. Liang, M. Hada, M. Ehara, K. Toyota, R. Fukuda, J. Hasegawa, M. Ishida, T. Nakajima, Y. Honda, O. Kitao, H. Nakai, T. Vreven, K. Throssell, J. A. Montgomery, Jr., J. E. Peralta, F. Ogliaro, M. J. Bearpark, J. J. Heyd, E. N. Brothers, K. N. Kudin,V. N. Staroverov, T. A. Keith, R. Kobayashi, J. Normand, K. Raghavachari, A. P. Rendell, J. C. Burant, S. S. Iyengar, J. Tomasi, M. Cossi, J. M. Millam, M. Klene, C. Adamo, R. Cammi, J. W. Ochterski, R. L. Martin, K. Morokuma, O. Farkas, J. B. Foresman, and D. J. Fox, Gaussian, Inc., Wallingford CT, 2019.
25 I. Funes-Ardoiz and R. S. Paton, GoodVibes (v3.0.0), Zenodo, 2019, https://doi.org/10.5281/zenodo.33461662018.
26 J. C. M. Monbaliu and P. Bianchi, SnapPy (v1.0.0), Zenodo, 2023, https://doi.org/10.5281/zenodo.8116089.
27 L. R. Domingo, M. Ríos-Gutiérrez and P. Pérez, *Molecules*, 2106, **21**, DOI:10.3390/molecules21060748.
28 P. Geerlings, F. De Proft and W. Langenaeker, *Chem. Rev.*, 2003, **103**, 1793–1873.
29 T. Klöffel, D. Gordon, S. Popiel, J. Nawala, B. Meyer and P. Rodziewicz, *Process Saf. Environ. Prot.*, 2023, **172**, 105–112.
30 Q. E. Thompson, *J. Am. Chem. Soc.*, 1961, **845**, 845–851.
31 K. D. Nagy, B. Shen, T. F. Jamison and K. F. Jensen, *Org. Process Res. Dev.*, 2012, **16**, 976–981.
32 L. Wan, M. Jiang, D. Cheng, M. Liu and F. Chen, *React. Chem. Eng.*, 2022, **7**, 490–550.
33 M. Vaz, D. Courboin, M. Winter and P. M. C. Roth, *Org. Process Res. Dev.*, 2021, **25**, 1589–1597.
34 D. Polterauer, D. M. Roberge, P. Hanselmann, P. Elsner, C. A. Hone and C. O. Kappe, *React. Chem. Eng.*, 2021, **6**, 2253–2258.
35 F. Lou, Q. Cao, C. Zhang, N. Ai, Q. Wang and J. Zhang, *J. Flow Chem.*, 2022, **12**, 307–315.
36 K. Lee, H. Lin and K. F. Jensen, *React. Chem. Eng.*, 2017, **2**, 696–702.
37 M. Irfan, T. N. Glasnov and C. O. Kappe, *Org. Lett.*, 2011, **13**, 984–987.
38 M. J. Nieves-Remacha and K. F. Jensen, *J. Flow Chem.*, 2015, **5**, 160–165.
39 M. O'Brien, I. R. Baxendale and S. V. Ley, *Org. Lett.*, 2010, **12**, 1596–1598.